Contrast in scanning probe microscopy images of ultra-thin insulator films

Andreas Klust,[1,*] Taisuke Ohta,[2,†] Markus Bierkandt,[3] Carsten Deiter,[3] Qiuming Yu,[1] Joachim Wollschläger,[3] Fumio S. Ohuchi,[2] and Marjorie A. Olmstead[1]

[1] *University of Washington, Department of Physics, Seattle, WA, USA*
[2] *University of Washington, Department of Materials Science and Engineering, Seattle, WA, USA*
[3] *Institut für Festkörperphysik, Universität Hannover, Hannover, Germany*

(Dated: June 20, 2005)

The contrast in scanning probe microscopy (SPM) images of ultra-thin CaF_2 films epitaxially grown on Si(111) is studied using scanning tunneling microscopy (STM) and scanning force microscopy (SFM). STM images of CaF_2/Si(111) exhibit a distinct contrast depending on the bias voltage. While images obtained with positive sample bias voltages show the physical topography of the film, images obtained with negative voltages either do not show CaF_2 islands or image them as depressions (contrast inversion) at high negative bias voltages (exceeding -8 V). Using SFM, CaF_2 can be distinguished from the underlying Si-CaF interface layer by measuring the dissipation of the cantilever oscillation caused by the contact potential difference between CaF_2 and the CaF bilayer.

PACS numbers: 68.37.Ef, 68.37.Ps, 68.55.-a, 73.40.Cg
Keywords: scanning tunneling microscopy (STM), scanning force microscopy (SFM), insulator films, material contrast

Thin insulator films grown on semiconductor or metal substrates are becoming increasingly important for both applications and basic research. For instance, insulator films are used as tunneling barriers in electronic device applications or gate dielectrics in field effect transistors. Insulators also play an important role in catalysis both as active material and as support for metal nanoparticles. Insulator films are frequently used instead of bulk samples to enable the study of surface properties of insulators with techniques that require conductive samples, such as scanning tunneling microscopy (STM) and various electron spectroscopies. STM can be used to study insulator films on conductive substrates if the insulator is thin enough to allow electrons to pass the film by ballistic transport or tunneling. For a recent review, see Ref. 1 and references therein.

Contrast in STM images of insulator films does not necessarily reflect the film morphology.[1, 2] It is influenced by a wide variety of effects, including the electronic structure of the substrate, insulator film, and/or interface between them, band-bending effects induced by the electric field between tip and sample, field resonances, and image potential states. This complicates the interpretation of STM images. Nevertheless, STM is not only an invaluable tool to image insulating films but the strong influence of the insulator electronic structure on image contrast can be utilized to obtain additional information, e.g. contrast between different chemical species.[3]

CaF_2 is an ionic material with a large band-gap of 12 eV. The small lattice misfit with Si (0.6% at room temperature) makes it a model system for epitaxial growth and a promising material for tunnelling barriers.[4, 5] The most stable configuration of the interface is a bilayer with CaF stoichiometry that is overgrown by bulk-like CaF_2.[5–7] Several studies employed STM to study CaF_2 films grown on semiconductors[3, 8–10] or metals[11]. Friction force microscopy can also be used to distinguish the CaF bilayer from CaF_2.[12] In this letter, we present a systematic investigation of the contrast in scanning probe microscopy (SPM) images of ultra-thin CaF_2/Si(111) films using both STM and scanning force microscopy (SFM).

Si samples were cut from boron-doped Si(111) and degassed for >12 h at ∼600 °C after insertion into ultra-high vacuum (UHV). The native oxide was removed by flash-annealing the samples to ∼1200 °C. The samples were then annealed at 900 °C for 10 min and finally slowly cooled to room temperature. The quality of the Si(111)-(7×7) reconstruction was checked by STM. CaF_2 films were grown by molecular beam epitaxy (MBE), depositing 1.5 TL CaF_2 on Si at 600 °C with a deposition rate of 0.5 TL CaF_2 per min (One triple-layer [TL] consists of $7.8 \cdot 10^{14}$ CaF_2 molecules/cm^2.). Under these growth conditions, the Si substrate is initially covered by a CaF bilayer which completely covers the substrate until CaF_2 islands nucleate on top of this CaF bilayer.[13, 14]

All STM images presented in this letter were acquired in the constant current mode. The values given for the bias voltage are with respect to the sample. Dynamic SFM images were acquired using the frequency modulation technique.[15] We used Si cantilevers with a resonant frequency of ∼280 kHz and a constant vibration amplitude A of ∼10 nm. The dissipation, i.e. the excitation amplitude required to keep A constant, was measured simultaneously with the topography. The influence of electrostatic forces between tip and sample was minimized by applying a bias voltage between tip and sample (see

*Electronic address: klust@fas.harvard.edu; Present address: Stanford University, Department of Chemical Engineering, Stanford, CA, USA
†Present address: Advanced Light Source, Lawrence Berkeley National Laboratory, Berkeley, CA.

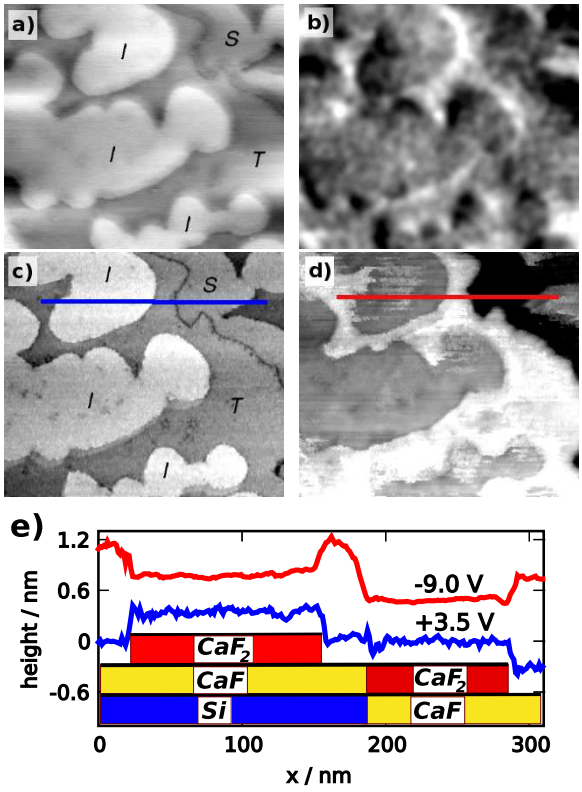

FIG. 1: (color online) SPM micrographs obtained with different SPM techniques showing the same region on the sample: a) dynamic SFM with $\Delta f = -500$ Hz, b) dissipation signal acquired simultaneously with a), c) dynamic cantilever STM with $U_{bias} = +3.5$ V and $I = 80$ pA, and d) static cantilever STM with $U_{bias} = -9.0$ V and $I = 80$ pA. All micrograph show areas of 400×350 nm^2. The topography images a), c), and d) use the same gray scale. The data shown in b) has been low-pass filtered to enhance the contrast. Linescans from c) and d) along the marked line are shown in e) together with a model of the film's cross-section.

Fig. 2).

SFM and STM images of the same sample area were obtained using the same Si cantilever for both SFM and STM measurements. For dynamic cantilever STM measurements,[16] the cantilever was externally excited at its resonant frequency (as in the SFM measurements) and images were acquired in constant tunneling current mode. The cantilever oscillation breaks down at relatively high bias voltages (<-5 V) during tip approach before a stable tunneling current can be measured. This break-down of the cantilever oscillation is caused by the high electrostatic forces in close proximity to the sample. Hence, we used static cantilever STM at high bias voltages. During static cantilever STM, the cantilever is not oscillated and is used in the same way as a standard metal STM tip. We observed no differences between STM images taken in this way and with standard tungsten metal tips.

The topography obtained by STM with positive bias voltage is practically identical to the topography observed by SFM (compare Fig. 1.a and c). The measured heights of identical features in both images are the same within the experimental uncertainties. All observed step heights of 0.3 nm in Fig. 1.a) and c) agree with the step height of 0.31 nm expected for both CaF_2(111) and Si(111). Therefore, we conclude that the STM image obtained with positive bias voltage shows the film morphology.

The contrast in STM images acquired with large negative bias voltage is inverted (see Fig. 1.d). The CaF_2 islands grown on the CaF bilayer marked with I are imaged as 0.2 nm deep depressions in the negative bias STM image, as opposed to 0.3 nm protrusions in the positive bias STM image (see Fig. 1.d and the model in Fig. 1.e) and in the SFM image (see Fig. 1.a). The same behavior is observed for the area marked with S which corresponds to a CaF_2 island adjacent to a step edge.

U_{bias}/V	H_1/ nm
+4.0	+0.29
+3.5	+0.32
−5.0	+0.08
−6.0	0
−7.0	0
−8.0	−0.21
−9.0	−0.20

TABLE I: Dependence of the apparent heights H_1 of first layer CaF_2 islands in constant current STM images on the bias voltage U_{bias}.

The apparent heights of CaF_2 grown on the CaF bilayer as measured by STM are listed for various bias voltages in Table I. We were unable to obtain stable STM images with bias voltages between roughly +3.0 and -5.0 V. The apparent step heights of CaF_2 islands on the CaF bilayer for positive bias voltages equals the geometric height of 0.31 nm of one molecular CaF_2(111) layer within the uncertainties of measurement.

The dissipation signal also allows discrimination between the CaF bilayer and CaF_2 islands (see Fig. 1.b). Although the contrast in the dissipation image is rather low, one can distinguish two different areas: i) the areas S and I (CaF_2 islands) with roughly the same dissipation and ii) T (CaF bilayer) with slightly higher dissipation.

SFM can be used to measure local differences in the contact potential between the SFM tip and the sample,[17, 18] by turning off the feedback loop controlling the tip-sample distance and measuring the bias voltage dependence of the cantilever's resonance frequency. Fig. 2 shows the change in cantilever resonant frequency as function of the bias voltage with the tip positioned over the CaF bilayer and over a CaF_2 island grown on the CaF bilayer. The change of the resonance frequency is proportional to $(U_{bias} - U_{CP})^2$ where U_{CP} represents the contact potential between tip and sample.[19] The contact potential difference is equal to the workfunction

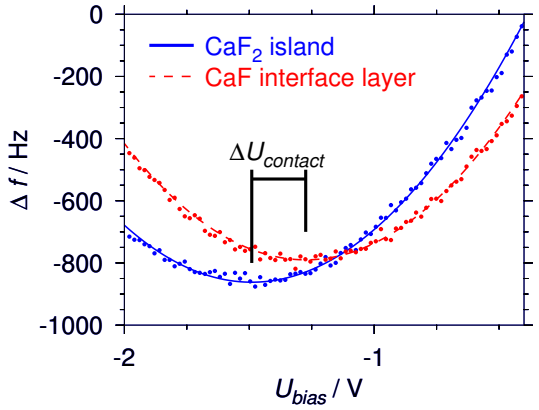

FIG. 2: (color online) Dependence of the frequency shift Δf as measured by scanning force spectroscopy on the bias voltage U_{bias} applied between tip and sample for the CaF bilayer and a CaF_2 island on top of the CaF bilayer. The lines show least-square fits of the data.

difference between the CaF bilayer and the one TL high CaF_2 islands grown on top of it. The CaF bilayer has a 0.22 eV higher workfunction than CaF_2 islands.

This workfunction difference reflects a difference in the electric field between the tip and sample between positioning the tip over the CaF bilayer (region T in Fig. 1) or over CaF_2 islands (regions I and S in Fig. 1). We suggest that these changes in the electric field cause the material contrast in the dissipation signal shown in Fig. 1(b) by Joule dissipation.[20]

STM has been widely used to investigate thin oxide films on metal substrates. For instance, CoO islands on Ag(001) have been imaged as depressions for tunnelling bias voltages between -1.5 and +2.2 V and as protrusions for voltages outside this range.[2] Similar behavior was found for several oxides grown on metals as recently reviewed by Schintke and Schneider.[1] The strong dependence of the apparent height of insulator islands on metals on the bias voltage is generally attributed to the band-gap of the insulator: Bias voltages within the band-gap cause tunnelling from/into the metal substrate through the insulator resulting in negligible or even negative apparent heights. Bias voltages outside this range cause tunnelling into the oxide's conduction band or from the oxide's valence band resulting in positive apparent heights.

The p-type Si substrate has a 1.1 eV band-gap with the Fermi-level pinned close to the valence band maximum (VBM). The valence band offset between Si and CaF_2 is in the range of 7.3 to 8.3 eV.[21] Therefore, considering the CaF_2 band gap of 12.1 eV one expects the conduction band minimum (CBM) of the CaF_2 film between 2.7 and 3.7 eV above the Si CBM. The bias voltage of +3.5 V used to acquire the positive bias voltage STM images is high enough to inject electrons from the tip into the CaF_2 conduction band. This explains the normal contrast observed in STM images obtained with positive sample bias voltages, where the images reflect the sample morphology as well as the difficulties in obtaining stable STM images with positive bias voltages below +3 V. The contrast inversion for bias voltages $\leq$-8 V, however, cannot be explained with tunneling from the CaF_2 valence band. In the absence of band bending and field emission this voltage should be high enough for tunneling from the valence band leading to normal contrast. The observed inverted contrast at high negative bias voltages, however, suggests that field emission dominates the tunneling current. Assuming that the electrons contributing to the current do not come from the CaF_2 film but from the interface region the contrast inversion can be explained by a dampening of the current by the CaF_2 film.

It is quite surprising that stable imaging of CaF_2 films grown on Si can be routinely achieved with bias voltages as high as -9 V. Usually, bias voltages in this range are used for tip cleaning and do not allow stable images. For instance, dielectric breakdown is reported for Al_2O_3/NiAl(110) films[22] at lower electric fields than routinely used by us for STM imaging. We suggest that the high band-gap of CaF_2 and stable interface between CaF_2 and Si contribute to the stability of STM at these unusually high voltages.

This work is supported by the U.S. Department of Energy grant no. DE-FG03-97ER45646, the M. J. Murdock Charitable Fund, and the Deutsche Forschungsgemeinschaft grant no. Wo 533/6. A.K. further gratefully acknowledges support by the Alexander von Humboldt-Foundation and T.O. financial support from the University Initiative Fund of the University of Washington.

[1] S. Schintke and W.-D. Schneider, J. Phys.: Condens. Matter **16**, R49 (2004).
[2] C. Hagendorf, R. Shantyr, K. Meinel, K.-M. Schindler, and H. Neddermeyer, Surf. Sci. **532-535**, 346 (2003).
[3] J. Viernow, D. Y. Petrovykh, A. Kirakosian, J.-L. Lin, F. K. Men, M. Henzler, and F. J. Himpsel, Phys. Rev. B **59**, 10356 (1999).
[4] L. J. Schowalter and R. W. Fathauer, CRC Critical Reviews in Solid State and Materials Science **15**, 367 (1989).
[5] M. A. Olmstead, *Thin Films: Heteroepitaxial Systems* (World Scientific Publishing, Singapore, 1999), chap. Heteroepitaxy of Strongly Disparate Materials: From Chemisorption to Epitaxy in CaF_2/Si(111), pp. 211–266.
[6] R. M. Tromp and M. C. Reuter, Phys. Rev. Lett. **61**, 1756 (1988).
[7] A. Klust, M. Bierkandt, J. Wollschläger, B. H. Müller, T. Schmidt, and J. Falta, Phys. Rev. B **65**, 193404 (2002).
[8] P. Avouris and R. Wolkow, Appl. Phys. Lett. **55**, 1074 (1989).

[9] T. Sumiya, T. Miura, and S. Tanaka, Surf. Sci. **357-358**, 896 (1996).
[10] K. Kametani, K. Sudoh, and H. Iwasaki, Jpn. J. Appl. Phys. Part 1 **41**, 250 (2002).
[11] F. Calleja, J. J. Hinarejos, A. L. Vzquez de Parga, S. M. Suturin, N. S. Sokolov, and R. Miranda, Surf. Sci. **582**, 14 (2005).
[12] A. Klust, H. Pietsch, and J. Wollschläger, Appl. Phys. Lett. **73**, 1967 (1998).
[13] U. Hessinger, M. Leskovar, and M. A. Olmstead, Phys. Rev. Lett. **75**, 2380 (1995).
[14] A. Klust, R. Kayser, and J. Wollschläger, Phys. Rev. B **62**, 2158 (2000).
[15] T. R. Albrecht, P. Grütter, D. Horne, and D. Rugar, J. Appl. Phys. **69**, 668 (1991).
[16] M. Guggisberg, M. Bammerlin, R. Lüthi, C. Loppacher, F. Battiston, J. Lü, A. Baratoff, E. Meyer, and H.-J. Güntherodt, Appl. Phys. A **66**, S245 (1998).
[17] N. Nonnenmacher, M. P. O'Boyle, and H. K. Wickramasinghe, Appl. Phys. Lett. **58**, 2921 (1991).
[18] J. Lü, M. Guggisberg, R. Lüthi, M. Kubon, L. Scandella, C. Gerber, E. Meyer, and H.-J. Güntherodt, Appl. Phys. A **66**, S273 (1998).
[19] M. Guggisberg, M. Bammerlin, C. Loppacher, O. Pfeiffer, A. Abdurixit, V. Barwich, R. Bennewitz, A. Baratoff, E. Meyer, and H.-J. Güntherodt, Phys. Rev. B **61**, 11151 (2000).
[20] W. Denk and D. W. Pohl, Appl. Phys. Lett. **59**, 2171 (1991).
[21] M. A. Olmstead, R. I. G. Uhrberg, R. D. Bringans, and R. Z. Bachrach, Phys. Rev. B **35**, 7526 (1987).
[22] C. Niu, N. P. Magtoto, and J. A. Kelber, J. Vac. Sci. Tech. **19**, 1947 (2000).